



Palladium on carbon-catalysed carbon-carbon coupling reactions of cyclohexanone (KA oil) and alkyl alcohols for the synthesis of zero net emission jet fuels

Matea Bačić, Judit Oliver-Meseguer^{*}, Antonio Leyva-Pérez^{*}

Instituto de Tecnología Química (Universitat Politècnica de València- Agencia Estatal Consejo Superior de Investigaciones Científicas), Avda. de los Naranjos s/n, València 46022, Spain

ARTICLE INFO

Keywords:

Cyclohexanone
KA oil
Palladium catalysis
Heterogeneous catalysis
Zero net emission jet fuels

ABSTRACT

The cyclohexanone / cyclohexanol mixture (KA oil) is one of the most produced C₆ chemicals worldwide, derived from renewable sources if desired; however, the use of KA oil as a precursor for zero net emission fuels has not been studied in-depth yet, as far as we know. We show here that KA oil is converted to an aromatic-free product mixture compatible with the composition of jet fuels after a series of carbon-carbon coupling reactions, of either KA oil with itself or with bioderived alcohols, in the presence of a commercially available solid-supported palladium on carbon catalyst under basic conditions (KOH). Water is the only by-product of the reaction, and phosphines can be used as ligands to vary the final product composition.

1. Introduction

Zero net emission fuels are considered a practical alternative to current fossil-based fuels since they have a similar chemical composition and, thus, properties to the latter. Still, they do not contribute to global warming since CO₂ is adsorbed by the original source (i.e. plants) in the same amount emitted by the final sustainable fuel. However, it has to be said that this is only strictly true if the processing of these fuels (i.e., plants to fuel) is CO₂ emission free, which has to be taken into consideration when calculating the overall carbon footprint for the whole process. Nevertheless, despite renewable energies (H₂, photovoltaics, electric batteries,...) are superior in terms of overall carbon footprint, air transportation will still require the use of highly energetic fuel sources such as jet fuel or kerosene. Thus, the search for zero net emission jet fuels should be a priority from the global warming point of view, much more considering that the contribution of aeroplanes to the global transport CO₂ emissions can be as high as 14% [1]. Jet fuels are a mixture of hydrocarbons comprising molecules between 8 and 16 atoms, and cyclohexane derivatives are a typical major component of this mixture; thus the use of the cyclohexanone / cyclohexanol mixture (KA oil) as a starting material to prepare jet fuel seems a valid synthetic pathway. However, we could just find in the literature one single example of this approach, where different types of cycloketone

compounds (5 and 6-membered cycles) were employed to prepare decalin derivatives [2].

Fig. 1 shows that KA oil is produced industrially from benzene by hydrogenation to cyclohexane and later aerobic oxidation to KA oil [3]. The production of KA oil for 2023 is estimated to be ~8000 thousand tonnes worldwide. Half of this amount is destined for the fabrication of nylon 6,6 after preparing adipic acid with HNO₃ [4]. This is a highly contaminant process sought to be circumvented. Indeed, producing adipic acid directly from biomass sources is a hot topic of much research [5]. Not only adipic acid but also all the intermediates in the production chain of nylon 6,6 (in concrete, benzene, cyclohexane and KA oil) can be sustainably produced from renewable sources, despite it must be recognized that a cost effective and commercially available approach for bioderived benzene and cyclohexane is still to be found, thus they are still likely to be prepared from oil in the short term. Anyway, benzene can be obtained from lignin [6,7], fatty acids [8], bioalcohols [9,10] and methane derivatives (after CO₂ hydrogenation) [11,12]; cyclohexane can be obtained from bio-oils [13] and guaiacol [14]; and the same KA oil can be obtained from lignin and derivatives [2]. With this in mind, one could envision that KA oil will be produced at some point from renewable sources but that its fate will not be the production of adipic acid. Thus, other industrial production uses might be of interest. Here we propose the use of KA oil for the synthesis of jet fuel.

^{*} Corresponding authors.

E-mail addresses: joliverm@itq.upv.es (J. Oliver-Meseguer), anleyva@itq.upv.es (A. Leyva-Pérez).

<https://doi.org/10.1016/j.apcata.2024.119632>

Received 15 November 2023; Received in revised form 7 February 2024; Accepted 15 February 2024

Available online 16 February 2024

0926-860X/© 2024 The Author(s). Published by Elsevier B.V. This is an open access article under the CC BY-NC-ND license (<http://creativecommons.org/licenses/by-nc-nd/4.0/>).

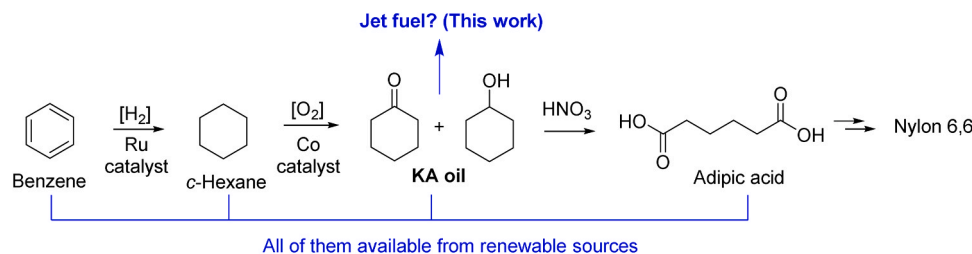


Fig. 1. Industrial synthesis of nylon 6,6 through KA oil, which can be diverted here to jet fuels.

2. Materials and methods

2.1. General

Reagents were obtained from commercial sources (Merck-Aldrich) and used without further purification otherwise indicated. Pd/C was obtained from different commercial sources (Merck Aldrich / ABCR / Stream chemicals) and used as received. The characteristics for these Pd/C solids can be found elsewhere [4], in particular, they were dried pre-reduced catalysts with 5 wt% Pd and rounded Pd nanoparticles of ~ 3 nm diameter size. Gas chromatography (GC) and gas chromatography coupled to mass spectrometry (GC-MS) were carried out in gas chromatographs with 25 m capillary columns filled with 1 or 5 wt% phenyl silicone (Shimadzu GC-2025, Agilent GC 6890 N coupled with Agilent MS5973). ^1H - and ^{13}C -nuclear magnetic resonance (NMR) were measured in CDCl_3 at room temperature on a 400 MHz spectrometer (Bruker Ascend 400), respectively, using Me_4Si as the internal standard. The metal content of the samples was determined by inductively coupled plasma-emission optical spectrophotometry (ICP-OES). Solids were disaggregated in *aqua regia* and later diluted in miliQ water before analysis. The Pd/C digestion solutions were centrifuged and filtered prior to analysis. ^{31}P solid state magic angle spinning nuclear magnetic resonance (MAS NMR) of the Pd/C sample containing PPh_3 was recorded in a Bruker Ascend 400WB, with a 90 pulse of 4 μs and a recycle delay of 20 s, spinning the sample at 20 kHz. The spectrum was referenced to H_3PO_4 (0 ppm).

2.2. PXRD measurements

Routine measurements were performed in Bragg-Brentano geometry using a PANalytical CUBIX diffractometer. X-ray radiation of $\text{Cu K}\alpha$ ($\lambda_1 = 1.5406 \text{ \AA}$, $\lambda_2 = 1.5444 \text{ \AA}$, $I_2/I_1 = 0.5$) was used, with a tube voltage and intensity of 45 kV and 40 mA respectively. The length of the arm of the goniometer was 200 mm, and a variable divergence slit with an irradiated sample area of 3 mm was used. The measurement range was from 2.0° to 90.0° (2θ), with a step of 0.020° (2θ) and a counting time of 17 seconds per step. The measurements were performed at 298 K, rotating the samples at 0.5 revolutions per second. In-situ measurements were performed in Bragg-Brentano geometry using an Anton Paar XRK-900 high temperature chamber installed in a PANalytical EMPYREAN diffractometer. X-ray radiation of $\text{Cu K}\alpha$ ($\lambda_1 = 1.5406 \text{ \AA}$, $\lambda_2 = 1.5444 \text{ \AA}$, $I_2/I_1 = 0.5$) was used, with a tube voltage and intensity of 45 kV and 40 mA, respectively. The length of the arm of the goniometer was 240 mm, and a fixed divergence slit with an aperture of $1/4^\circ$ was used. The measurement range was from 5° to 90.0° (2θ), with a step of 0.026° (2θ) and a counting time of 132 seconds per step. The measurements were performed at 298 K, rotating the samples at 0.5 revolutions per second, under a continuous flow of 10% H_2 in He.

2.3. CO adsorption

The dispersion of Pd in the catalyst was estimated from the adsorption of CO using the double isotherm method in a Quantachrome Autosorb-1 C equipment. The samples were diluted with silica to

prepare the pellet (60:40, sample: SiO_2). Before adsorption, the samples (300 mg with a pellet size of 0.8–1.1 mm) were degassed under vacuum, and then pure CO was supplied to measure the first adsorption isotherm (i.e. total CO adsorption). After evacuation to 25°C , the second isotherm (i.e. reversible CO adsorption) was recorded. The amount of chemisorbed CO was obtained by subtracting the two isotherms. The equations used for metal dispersion and metal diameter determination are $D(\%) = Nm \cdot Fs \cdot M \cdot 100 / L \cdot 100$, where Nm is the chemisorption adsorption expressed in mol of CO per gram of sample, Fs is adsorption stoichiometry, M is molecular weight of the supported metal and L is percentage of loading of the supported metal; $d = L \cdot 6 \text{ ASA} \cdot Z / 100$, where d is average diameter of the metal (nm), ASA is the active surface area ($\text{m}^2 \cdot \text{g}^{-1}$ of sample) calculated from the following equation: $\text{ASA} = Nm \cdot Fs \cdot A_m \cdot A_N$ (A_m is cross-sectional area occupied by each active surface atom and A_N is Avogadro's number) and Z is the density of the supported metal ($\text{g} \cdot \text{m}^{-3}$).

2.4. General reaction procedure

A typical reaction procedure is as follows: To a mixture of Pd/C (0.02 mmol), KOH (0.6 mmol), and PPh_3 (0.02–0.32 mmol) is added the ketone (2 mmol) and alcohol (4 mmol) under N_2 . All the batch reactions, in this work, were performed in 6 mL round-bottomed vials with 0.6 mL of reaction volume and a stirring magnet. The reaction mixture was magnetically stirred in a pre-heated oil bath at 100°C for 4 h. Aliquots were taken either by direct extraction through a reactor steel exit, or after stopping the reaction and taken from the supernatant. Filtration was carried out when some solid was present in the sample. The conversions and yields of products were estimated from the peak areas based on the internal standard technique using GC. GC-coupled mass spectrometry and NMR were used to identify the products, besides comparison with pure product samples.

2.5. Reuse of the catalyst

After cooling the reaction mixture, the solid catalyst was recovered by gravity filtration, rinse with alcohol for washing, weighted, and placed in a new vial for a subsequent use, re-calculating the amounts of reactants as a function of the new catalyst weight, to maintain the same relative amounts.

2.6. Hot filtration test

The kinetics of the reaction was followed by GC under optimized reaction conditions, and then the reaction was repeated under exactly the same reaction conditions but filtering the reaction mixture in hot through a $25 \mu\text{m}$ Teflon™ membrane filter, after 5 min reaction time (12% conversion), in order to remove the solid catalyst. The filtrates were placed in a previously heated vial at the same reaction temperature and magnetically stirred at the reaction temperature. The corresponding kinetics was followed by GC.

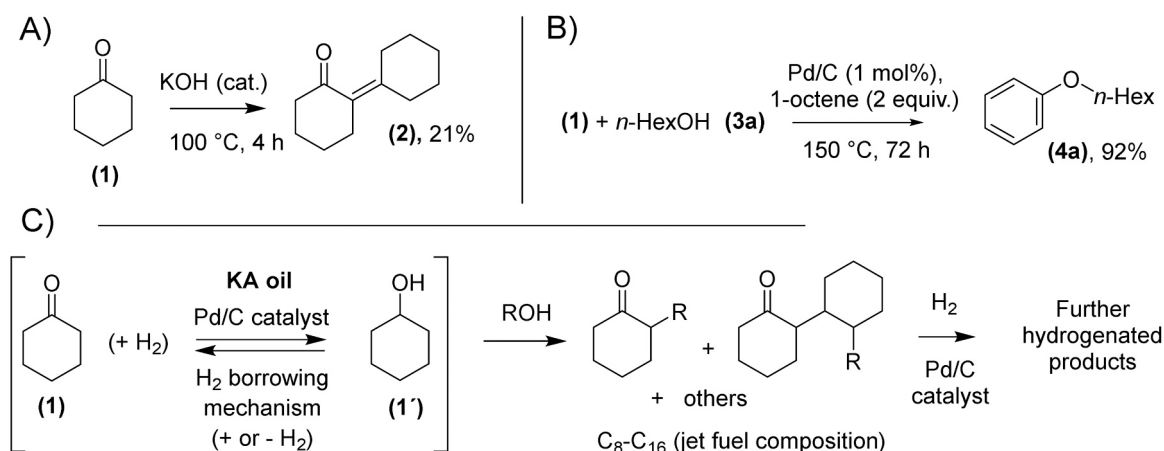


Fig. 2. Non-catalytic and catalytic strategies used here to prepare hydrocarbon compositions compatible with jet fuels.

2.7. In-situ hydrogenation reaction

After performing the cyclohexanone coupling reaction in a reinforced double-walled reactor, an additional 9 mol% of Pd/C was added to the mixture and the reactor was capped with a sealed tap equipped with an entrance vessel and coupled to a manometer. The vial was flushed twice with H₂ and left under H₂ atmosphere (30 bar). Then, the reaction was placed in a pre-heated oil bath at 200 °C and magnetically stirred for 48 h. The reaction mixture was analyzed as indicated above.

3. Results and discussion

3.1. Results with stoichiometric reagents

A simple aldol condensation reaction under basic stoichiometric conditions is the more obvious reaction to engage cyclohexanone (1) in carbon-carbon (C-C) coupling reactions and extend the carbon chain to acceptable fuel jet compositions. Fig. 2A shows that, in our hands, this approach works well; however, the final product (2) is an unsaturated ketone, unsuitable for fuel purposes. Besides, the use of stoichiometric

amounts of base made the procedure unattractive for scaling up, with increased environmental impact and higher costs due to the need for more raw materials and disposal of waste by-products, including neutralization steps. The use of lower amounts of base, less than 1 equivalent (catalytic), gave low conversions.

A second approach could consist in the coupling of cyclohexanone (1) with bio-based alcohols [15] through hydrogen-borrowing coupling reactions [16,17], as shown in Fig. 2B. This approach has been reported with palladium on carbon (Pd/C) as a catalyst and a sacrificial alkene (1-octene) as a stoichiometric reagent to trap the excess of H₂ generated during the reaction [18–20]. In our hands, the reaction of cyclohexanone 1 with *n*-hexanol (3a) under the reported conditions [18–20] gave a 92% of the aromatic anisole derivative (4a) (see Table S1 in the Supplementary Information for reaction details). The aromatised product is the major component of the final mixture without base, regardless of the use or not of the sacrificial alkene, and the C-O coupling reaction occurs almost exclusively, which is not suitable for producing a fuel hydrocarbon mixture (Tables S2-S3 and Figure S1). Both the undesired C-O coupling and aromatisation reactions occur within a wide range of alcohols and reaction conditions to give the corresponding anisole derivatives and/or C-O coupled compounds as major products in all cases.

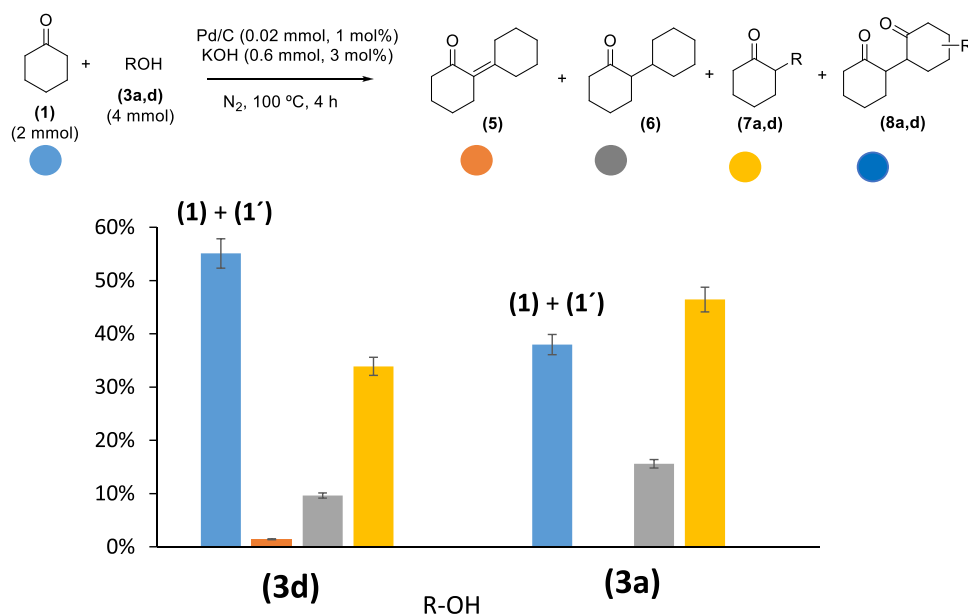


Fig. 3. Catalytic results for the alkylation of cyclohexanone (1) with *n*-hexanol 3a or *n*-propanol 3d using Pd/C and KOH as catalysts under the indicated reaction conditions. The remaining % of cyclohexanone (1) is a mixture with in-situ formed cyclohexanol (1') (KA oil). Error bars account for a 5% uncertainty.

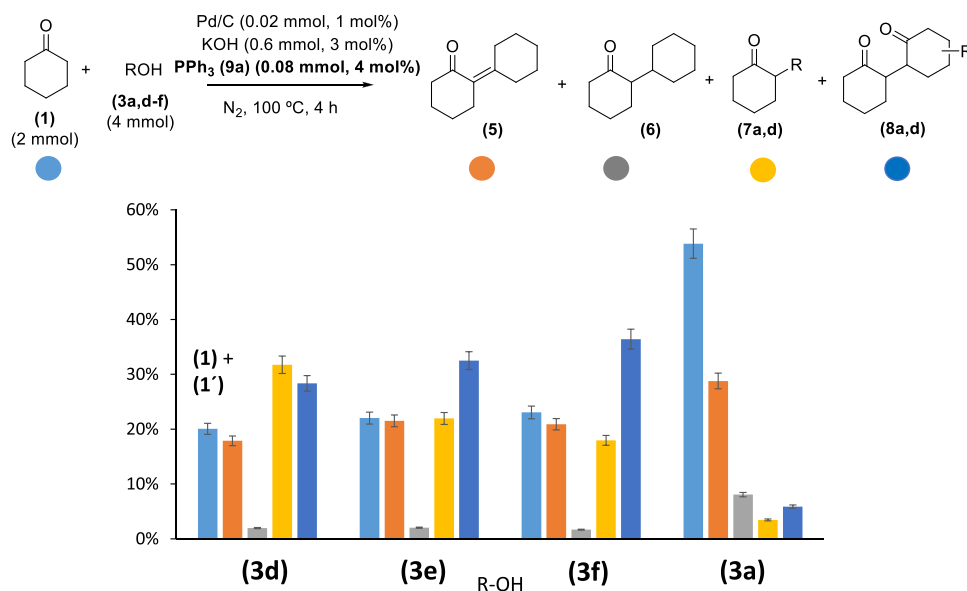


Fig. 4. Catalytic results for the alkylation of cyclohexanone (**1**) with the different alcohols **3a,d-f** using Pd/C and KOH as catalysts and PPh₃ **9a** as a ligand under the indicated reaction conditions. The remaining % of cyclohexanone (**1**) is a mixture with in-situ formed cyclohexanol (**1**) (KA oil). Error bars account for a 5% uncertainty.

Regarding the influence of the reaction atmosphere, in general, the conversion decreases with O₂. The reactions carried out under a nitrogen atmosphere tend to exhibit higher conversion rates compared to those performed under an oxygen atmosphere, despite the selectivity for the desired products may vary (please compare entries 1, 2, 5 and 6; and also 8 and 9, in Table S3).

Fig. 2C shows that, at this point, we envisioned that the reactions in Figs. 2A and 2B could be merged to promote the formation of saturated C-C bonds after ketone deprotonation, hydrogen-borrowed coupling reactions and concomitant hydrogenation reactions, in one-pot, without aromatizing the cyclohexanone product and by-passing the C-O coupled products [21,22]. For that, we just needed, in principle, to employ the Pd/C catalyst and KOH, also in catalytic (rather than stoichiometric like in Fig. 2A) amounts without the sacrificial alkene. In this way, the cyclohexanol (**1**) present in the KA oil mixture could also react, since (**1**) is in equilibrium with cyclohexanone (**1**) through the Pd-catalysed hydrogen-borrowing reaction [23]. Besides, as the only by-product is water, the same Pd/C catalyst will allow further hydrogenation of the product mixture with H₂ after the coupling reactions. The resulting product mixture is an aromatic-free and C-O-free hydrocarbon positions of potential use as a jet fuel.

3.2. Catalytic results without phosphines

Fig. 3 shows the results for the reaction between cyclohexanone (**1**) and *n*-hexanol **3a** or *n*-propanol **3d** catalysed by Pd/C (1 mol%) and KOH (3 mol%) after 4 h at 100 °C under an inert atmosphere, to minimize aromatisation reactions. The catalyst was the Pd/C (5 wt%) commercial sample employed for the reaction in Fig. 2B, which has an average Pd nanoparticle diameter size of ~1.7 nm according to high angle annular dark field scanning transmission electron microscopy (HAADF-STEM) imaging (Figure S2) and the corresponding powder X-ray diffractogram (PXRD), after applying the Scherrer equation (Figure S3) [4]. CO adsorption measurements confirmed the Pd nanoparticle dispersion on the solid catalyst. The dispersion of Pd (D) was calculated from the amount of CO irreversibly adsorbed, assuming a stoichiometry of Pd/CO = 1 [24–27]. The average diameter of the Pd nanoparticles (d) was determined from the chemisorption data assuming a spherical geometry for the metal particle according to the procedure described by Anderson [28]. A 78% overall palladium dispersion was

obtained, which corresponds to a 1.4 nm average particle size, in good agreement with the TEM measurements. This good dispersion, combined with the small particle size of the relatively highly loaded Pd solid catalyst, should enable the use of phosphines as ligands for further catalytic control (see ahead; unfortunately, the adsorption experiment did not work well after PPh₃ incorporation, probably due to the relative volatility of the latter, to the fact that the phosphine blocks the Pd surface and hinders CO adsorption, or to the weaker CO adsorption in the presence of the phosphine, to the point that the equilibrium coverage is far lower) [29]. Besides the commercial availability and wide use in industry of the Pd/C catalyst, the latter is very convenient for high-scale reaction productions [4].

It can be seen in Fig. 3 that neither aromatic, C-O coupled nor the unsaturated ketone **5** products are obtained when both alcohols (**3a**) and (**3d**) are used as reactants, but only the desired alkylated products **6** and **7** (**a** or **d**) in 45–60% yield, with a remarkable >75% selectivity to the ketone-alcohol coupled product **7** (**a** or **d**). These alkylated products fall within the specification of jet fuels (10–12 carbon hydrocarbons) and are particularly suitable for fueling purposes since they contain branched cyclohexane moieties.

The recovered cyclohexanone (**1**) is mixed with in-situ formed cyclohexanol (**1**), thus a KA oil composition. Kinetic experiments under exactly the same reaction conditions in Fig. 3 but with either simulated KA oil mixture or neat cyclohexanol (**1**) confirms the reactivity of both to give alkylated products, although with lower selectivity (Figures S4 and S5). The kinetic plot for the KA oil mixture (Figure S5) shows that cyclohexanone (**1**) reacts faster than cyclohexanol (**1**), which indicates that the alkylation reaction is somewhat faster than the hydrogen-borrowing reaction between (**1**) and (**1**). Nevertheless, the kinetic plot for neat (**1**) (Figure S5) confirms that both starting materials are inter-converted during the reaction. If the base is not employed as a catalyst, the interconversion between (**1**) and (**1**) still occurs, but the coupling products are barely formed even after prolonged times (6 h reaction time, Figure S6), which is in good agreement with the expected role of each catalyst, i.e. Pd/C to trigger the hydrogen-borrowing reactions and KOH to activate the alpha carbon atom of the ketone. Please notice that a significant further transformation from (**1**) to (**1**) does not occur when there are equal amounts of (**1**) and (**1**) from the beginning (Figure S7). This might be explained by an initial competitive absorption of (**1**), which may inhibit further reactivity of (**1**), and indicates that there is a

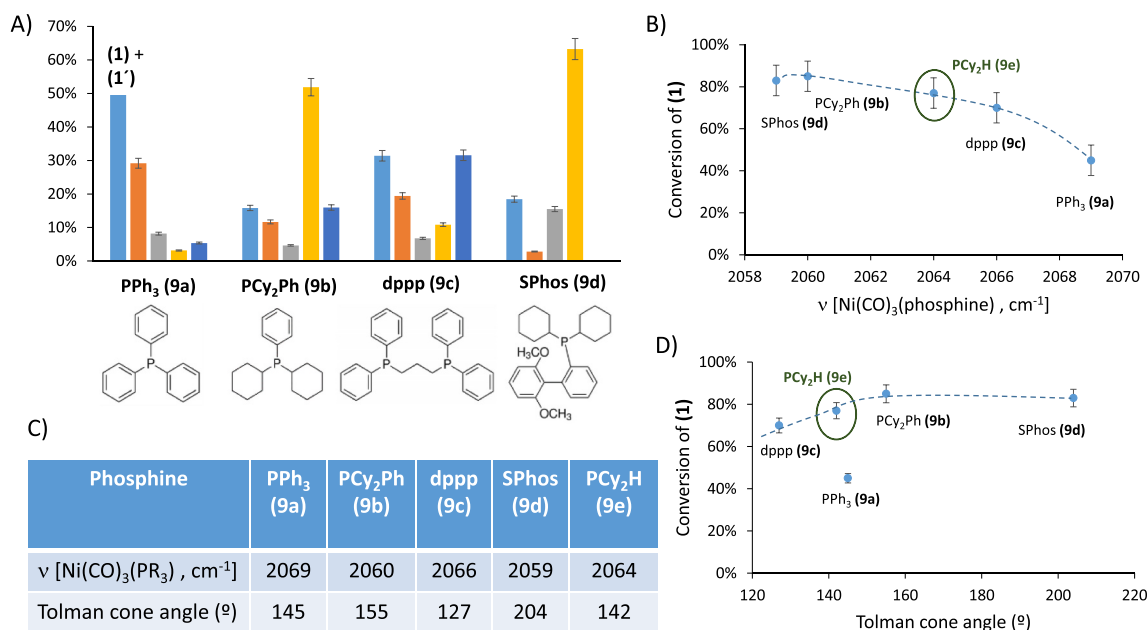


Fig. 5. A) Catalytic results for different phosphines during the alkylation of cyclohexanone (1) with alcohol 3a under the reaction conditions in Fig. 4 above. The remaining % of cyclohexanone (1) is a mixture with in-situ formed cyclohexanol (1') (KA oil). Error bars account for a 5% uncertainty. B) Correlation between the conversion of (1) and the phosphine electronic properties, expressed in terms of $\nu(\text{CO}, \text{cm}^{-1})$ of the corresponding $\text{Ni}(\text{CO})_3(\text{PR}_3)$ complex. C) Electronic and steric values for the different phosphines (9a-e) [29,40,41]. D) Correlation between the conversion of (1) and the phosphine Tolman cone angle.

balance between the rate of conversion from (1) to (1) and the reverse reaction. Further kinetic experiments with different relative amounts of (1) and (1'), with and without base (Figures S8 and S9), show that the interconversion between both occur in the presence of base, regardless the initial relative amount of (1) and (1'). The fact that neat (1) transforms to (1) without base could be tentatively explained by the formation of some active deprotonated species in the complete absence of starting (1) (Figure S6).

The Pd/C catalyst could be recovered from the reaction mixture and reused three times with slight loss of catalytic activity and selectivity throughout the reuses (Figure S10). In accordance, a hot filtration test shows that some catalytic species (<20%, considering also the blank experiment) are present in solution (Figure S11, top). Please notice that the increasing conversion after filtration in Figure S11 (orange line) nearly matches the blank experiment, i.e. the residual conversion with base and without palladium catalyst (grey line), which indicates that just minor catalytically active Pd species are leached into solution. We repeated again the hot filtration experiment, to confirm that a slight leaching occurs, which barely reflects in the final yield of the reaction (Figure S11, bottom). Inductively coupled plasma optical emission spectroscopy (ICP-OES) analyses of the spent Pd/C catalyst shows that up to 28% of the original supported Pd might be removed during reaction, and that the final Pd/C contains significant amounts (up to 5 wt%) of K on their structure, which obviously comes from the base employed during reaction. However, some loss of Pd and the incorporation of K (as K⁺) on the solid does not hamper the catalytic activity. This loss of palladium species during reaction could be palliated by palladium recovery after cooling, which is well-known in industry.

3.3. Catalytic results with phosphines as ligands

The interaction of phosphines with Pd nanoparticles was studied twenty years ago [30–36]; however, their catalytic implications have been only recently studied, mainly for hydrogenation [29,32–36] and cross-coupling reactions [37], but scarcely for other reactions [38]. In particular, we could not find any example of phosphine-ligated catalytic palladium nanoparticles for hydrogen-borrowing coupling reactions.

Fig. 4 shows the results for the reaction between cyclohexanone (1) and different alcohols under exactly the same conditions as above (Fig. 3) but employing, in this case, triphenylphosphine (9a) (PPh₃, 4 mol%) as a ligand for Pd/C. As it can be seen, the use of phosphine (9a) as a ligand produces an entirely different distribution of products, being the products (8) coupled to both the ketone (1) and the alcohol (3), the major one in most cases. Notice here that the alkyl substituent in products (8) can be in different positions of the cyclohexane moieties, which is indicated with an undefined bond. It is also noticeable the appearance of the unsaturated ketone (5) in significant amounts, which indicates that most of the reactive H₂ released from the hydrogen-borrowing events (i.e. from alcohols (3)) is now being consumed during the couplings of (1) and (6) with (3), in contrast with the reactions where phosphines are not present (see Fig. 3 above). A new experiment starting from neat (5) and (3a) shows that product (8a) is barely formed (Figure S12), which supports the necessity of the hydrogen-borrowing mechanism to occur, beyond the deprotonation reaction, for further C-C couplings to proceed. The influence in the reaction rate of the relative amounts of reagents (1), (3a) and phosphine ligand (9a) was studied by kinetic experiments (Figures S13–S14). The use of a two-fold amount of alcohol (3a) increases the reaction rate (Figure S13), and the maximum rate is found for a 4 mol% of phosphine (9a) (Figure S14). The reaction rate may also be increased here with the phosphine amount (see Figure S13, bottom left kinetics). Overall, phosphine (9a) as a ligand allows to obtain heavier fuel jet compositions since longer alkylated and saturated hydrocarbon chains (up to 17 carbon atoms, i.e. 8 f) can be prepared.

Different phosphines [(9b–d)] were then tested for the reaction with *n*-hexanol (3a), the less reactive alcohol, according to the results shown in Fig. 4 above. Notice that using an inert atmosphere and the continuous generation of hydrides during the reaction assure that phosphines will not be significantly oxidised and can be used safely as ligands for Pd/C. The presence of hydrides was confirmed by the clear shifting of the signal at 40° in PXRD experiments of the fresh catalyst sample, after exposition to H₂ atmosphere, in the presence or not of PPh₃ (Figure S15), and also by previous reports on RAMAN-IR [29]. The peak at 27° in PXRD (see also Figure S3), which corresponds to C support, decreases in

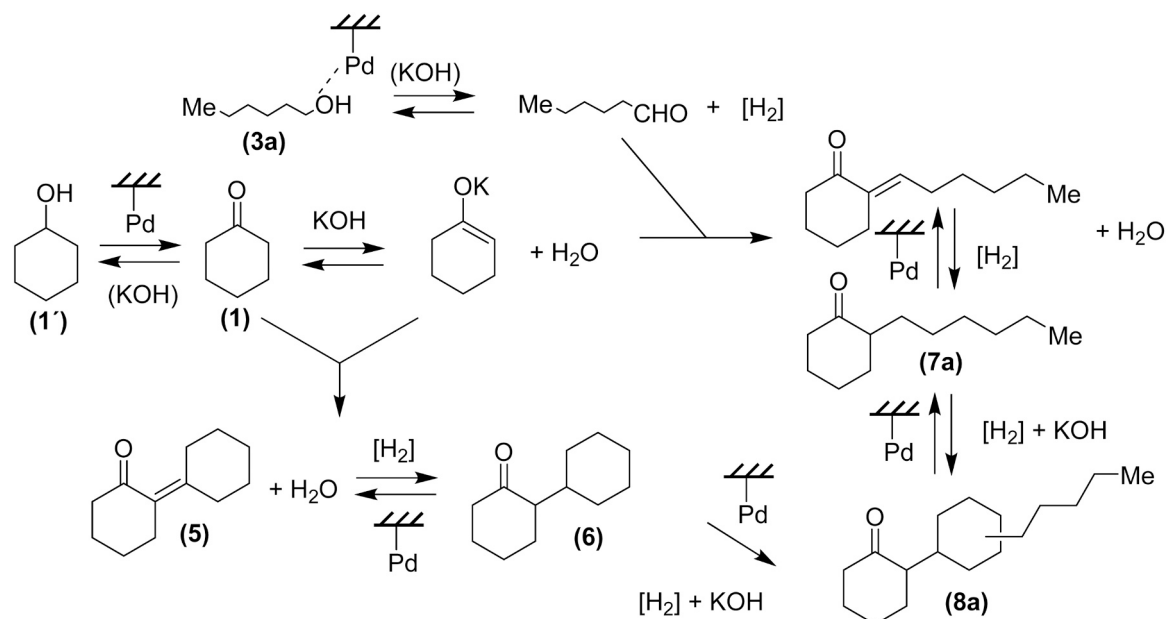


Fig. 6. Tentative mechanism for the Pd/C-KOH catalysed coupling reactions of KA oil with *n*-hexanol. Phosphines are ligated to Pd/C when used (omitted for the sake of clarity). [H₂] refers to Pd-H species.

the presence of PPh₃, probably because the peaks of the latter are much more intense. Notice that the phosphine is in excess respect to Pd, so there is free phosphine that can be adsorbed on the support. Since all other evidences point to the persistence of the Pd nanoparticles crystallinity after phosphine adsorption, we must accept that the decrease in the intensity of the C peak ($2\theta = 27^\circ$) occurs after phosphine addition. The new diffraction peaks after adsorption of PPh₃ just appear in the region of diffraction angles of 25–40°, shifted respect to the free PPh₃. Nevertheless, not all the phosphine is adsorbed into the catalyst and minor amounts can be oxidized during reaction, as confirmed by GC-MS analysis of the reaction mixture (Figure S16). Other differences respect to the PXRD of the fresh sample (See Figure S3) can be due to the use of different measurement conditions.

Fig. 5A shows the comparative catalytic results for the different phosphines, together with their chemical structure. Phosphines (9a–d) were selected in order to cover a wide range of electronic and steric properties, with different accepting-donating capabilities, parametrised as the vibrational frequency of the carbonyl stretch of the corresponding Ni(CO)₃(phosphine) complex (from 2059 to 2069 cm⁻¹), which correlates to the phosphine lone pair charge density [39], as well as cone angles ranging from 127° (1,3-bis(diphenylphosphino)propane, dppp 9c) to 205° (2-dicyclohexylphosphino-2',6'-dimethoxybiphenyl, SPhos 9d) [40,41].

The catalytic results show that the phosphine's nature strongly influences the conversion of (1) and the product distribution of the reaction. Fig. 5B shows that the conversion of (1) decreases as the phosphine electronic density does, nearly linearly. Indeed, the catalytic result for a totally different phosphine to those tested, i.e. secondary dicyclohexyl phosphine (9e), fitted perfectly in that correlation (circled in green in Fig. 5B). Fig. 5C tabulates the electronic parameters and the Tolman cone angles for the phosphines (9a–e), and while a catalytic activity-phosphine electronics relationship was found (Fig. 5B), the phosphine sterics seems to be irrelevant for the conversion of (1), as indicated by the correlation shown in Fig. 5D. Phosphine 9e was tested to check the validity of this correlation and fitted well (green circle).

The use of a simulated KA oil mixture under phosphine (9a)-catalysed conditions confirmed the catalytic activity in the KA oil mixture (Figure S17) and, as occurred for the reaction without phosphines, the presence of the base is necessary for the coupling reactions to proceed (Figure S18). Remarkably, the Pd/C-PPh₃ (9a) catalyst can be recovered

and reused without activity losses (Figure S19), and without the need of adding any additional phosphine throughout the reuses (Figure S20). These results indicate that the percentage of phosphine anchored to Pd/C from the beginning is the one doing the catalysis throughout the reuses. The solvent-free catalytic system reported here is amenable to being easily scaled up since Pd/C, KOH and phosphine (9a) are widely available commercial chemicals, Pd/C can be reused, and water is the only by-product of the reaction. Thus, a reaction at 10 times gram scale was performed, and the results were similar to those obtained at lower scales (Figure S21), thus confirming the easy scalability of the process. These results support the potential use of the Pd/C-PPh₃ (9a) solid as a truly recoverable and reusable catalyst for this reaction. We also tested the complex Pd(PPh₃)₄ as a catalyst for the reaction, and while a high conversion was observed, a plethora of products were found and any Pd could not be recovered from the reaction. Thus, despite it is true that some leached Pd could be acting during reaction, the advantage of our system is that we can recover most of the Pd (and some phosphine, see Figure S20) after reaction, and use the metal catalyst again. Notice that the supporting of the phosphine on the Pd/C catalyst has been confirmed by ³¹P solid state magic angle spinning nuclear magnetic resonance (MAS NMR, Figure S22) [29], since the new ³¹P chemical shift value for the solid catalyst is different and falls within the ³¹P values for either PPh₃ (solid-state NMR) [42], Pd(PPh₂)Cl₂ (solid-state NMR) [42], Pd(PPh₃)₄ (in CDCl₃) [43] or PPh₃O (in CDCl₃) [44].

Noble metals supported on carbon, including Pd/C, are able to catalyse the hydrogenation reaction not only of alkenes but also of carbonyl groups [4,45]. Thus, in principle, the obtained hydrocarbon mixture constituted by (1), (1) and (5–8) could be further hydrogenated, in-situ, by simply setting an atmosphere of H₂ after the coupling reactions, and continuing the reaction. Indeed, we were able to in-situ hydrogenate the remaining alkene and carbonyl groups, after adding additional Pd/C catalyst and setting 30 bars of H₂ at 200 °C for 48 h, to achieve a further C₆-C₁₈ saturated hydrocarbon mixture mainly composed by bicyclohexyl (53.7%), and free of aromatics and C-O ether bonds (Figure S23). The overall process constitutes a potential route for the synthesis of chemical mixtures compatible with a jet fuel composition [46].

A tentative reaction mechanism for the coupling of cyclohexanone (1) and *n*-hexanol (3a) is shown in Fig. 6. The alcohol is transformed to the corresponding aldehyde by a hydrogen-borrowing mechanism

catalysed by the (phosphine) Pd/C catalyst, probably also assisted by the catalytic base. Concomitantly, (1) is deprotonated by the base and the alkoxide intermediate couples with the aldehyde to give (7a) after hydrogenation of the alkene. Parallely, products (5) and (6) are formed by the same reaction pathway but exclusively with (1). (1) and (1) are interconverted during the process. Finally, product (8a) is formed by a new hydrogen-borrowing /deprotonation reaction sequence either over (6) or (7a). Notice that the (phosphine) Pd/C and KOH catalysts intervene in at least 5 steps during the reaction and that the only by-product is water, showcasing the catalytic process's efficiency and sustainability.

The released hydrogen atoms, depicted as [H₂] in the proposed mechanism, do not necessarily correspond to free H₂ but more probably to Pd-H species, ready to be transferred to the new products, which is supported by the lack of reactivity of (5) when used as the starting material (Figure S10). To confirm this point, product (6) was also used as the starting material during the reaction and, in contrast to (5), triggered the formation of products (8) (Figure S24). These results strongly support the hydrogen-borrowing /deprotonation reaction sequence proposed above.

4. Conclusions

Cyclohexanone (also KA oil) and bio-based alcohols react in the presence of catalytic amounts of Pd/C and KOH to give hydrocarbon mixtures of potential use as jet fuels. The process is solvent-free, gives water as the only by-product, and the Pd/C catalyst is recovered and reused. Phosphines can be used as ligands to modulate the hydrogen-borrowing reaction and, thus, the final product distribution. The resulting catalytic process can be considered as an efficient and sustainable system to give an aromatic-free, zero net emission jet fuel, potentially implementable at higher scales.

CRedit authorship contribution statement

Oliver-Meseguer Judit: Writing – review & editing, Writing – original draft, Validation, Supervision, Investigation, Funding acquisition, Formal analysis. **Bačić Matea:** Validation, Methodology, Investigation, Formal analysis. **Leyva-Pérez Antonio:** Writing – review & editing, Writing – original draft, Validation, Supervision, Resources, Project administration, Investigation, Funding acquisition, Conceptualization.

Declaration of Competing Interest

The authors declare that they have no known competing financial interests or personal relationships that could have appeared to influence the work reported in this paper.

Data availability

Data will be made available on request.

Acknowledgements

Financial support of the Spanish projects PID2020–115100GB–I00 and Ramón y Cajal contract number RYC2022–036154–I (both funded by MCIINN, the formed by the former by MCIN/AEI/10.13039/501100011033MICIIN) are also acknowledged. Financial support by Severo Ochoa centre of excellence program (CEX2021–001230–S) is gratefully acknowledged. M. B. thanks the ITQ for the concession of a contract. We thank Dr. J. L. Jordá for performing the H₂ atmosphere-PXRD experiments.

Appendix A. Supporting information

Supplementary data associated with this article can be found in the

online version at [doi:10.1016/j.apcata.2024.119632](https://doi.org/10.1016/j.apcata.2024.119632).

References

- https://climate.ec.europa.eu/eu-action/transport/reducing-emissions-aviation_en.
- R. Wang, G. Li, H. Tang, A. Wang, G. Xu, Y. Cong, X. Wang, T. Zhang, N. Li, Synthesis of decaline-type thermal-stable jet fuel additives with cycloketones, *ACS Sustain. Chem. Eng.* 7 (2019) 17354–17361, <https://doi.org/10.1021/acssuschemeng.9b04288>.
- W.-J. Zhou, R. Wischert, K. Xue, Y.-T. Zheng, B. Albela, L. Bonnevot, J.-M. Clacens, F. De Campo, M. Pera-Titus, P. Wu, Highly selective liquid-phase oxidation of cyclohexane to KA oil over Ti-MWW catalyst: evidence of formation of oxyl radicals, *ACS Catal.* 4 (2014) 53–62, <https://doi.org/10.1021/cs400757j>.
- P. Rubio-Marqués, J.C. Hernández-Garrido, A. Leyva-Pérez, A. Corma, One pot synthesis of cyclohexanone oxime from nitrobenzene using a bifunctional catalyst, *Chem. Commun.* 50 (2014) 1645–1647, <https://doi.org/10.1039/C3CC47693F>.
- W. Yan, G. Zhang, J. Wang, M. Liu, Y. Sun, Z. Zhou, W. Zhang, S. Zhang, X. Xu, J. Shen, X. Jin, Recent progress in adipic acid synthesis over heterogeneous catalysts, *Front. Chem.* 8 (2020) 00185, <https://doi.org/10.3389/fchem.2020.00185>.
- D. Wu, Q. Wang, O.V. Safonova, D.V. Peron, W. Zhou, Z. Yan, M. Marinova, A. Y. Khodakov, V.V. Ordomsky, Lignin compounds to monoaromatics: selective cleavage of C–O bonds over a brominated ruthenium Catalyst, *Angew. Chem. Int. Ed.* 60 (2021) 12513–12523, <https://doi.org/10.1002/anie.202101325>.
- Q. Meng, J. Yan, R. Wu, H. Liu, Y. Sun, N.N. Wu, J. Xiang, L. Zheng, J. Zhang, B. Han, Sustainable production of benzene from lignin, *Nat. Commun.* 12 (2021) 4534, <https://doi.org/10.1038/s41467-021-24780-8>.
- S. He, F.G.H. Klein, T.S. Kramer, A. Chandel, Z. Tegudeer, A. Heeres, H.J. Heeres, Catalytic conversion of free fatty acids to bio-based aromatics: a model investigation using oleic acid and an H-ZSM-5/Al₂O₃ catalyst, *ACS Sustain. Chem. Eng.* 9 (2021) 1128–1141, <https://doi.org/10.1021/acssuschemeng.0c06181>.
- V.C.S. Palla, D. Shee, S.K. Maity, Production of aromatics from n-butanol over HZSM-5, H-β, and γ-Al₂O₃: role of silica/alumina mole ratio and effect of pressure, *ACS Sustain. Chem. Eng.* 8 (2020) 15230–15242, <https://doi.org/10.1021/acssuschemeng.0c04888>.
- Q. Gong, T. Fang, Y. Xie, R. Zhang, M. Liu, F. Barzagli, J. Li, Z. Hu, Z. Zhu, High-Efficiency Conversion of Methanol to BTX Aromatics Over a Zn-Modified Nanosheet-HZSM-5 Zeolite, *Ind. Eng. Chem. Res.* 60 (2021) 1633–1641, <https://doi.org/10.1021/acs.iecr.0c06342>.
- S. Natesakhawat, N.C. Means, B.H. Howard, M. Smith, V. Abdelsayed, J.P. Baltrus, Y. Cheng, J.W. Lekse, D. Linka, B.D. Morreale, Improved benzene production from methane dehydroaromatization over Mo/HZSM-5 catalysts via hydrogen-permeable palladium membrane reactors, *Catal. Sci. Technol.* 5 (2015) 5023–5036, <https://doi.org/10.1039/C5CY00934K>.
- X. Fang, H. Liu, Z. Chen, Z. Liu, X. Ding, Y. Ni, W. Zhu, Z. Liu, Highly Enhanced Aromatics Selectivity by Coupling of Chloromethane and Carbon Monoxide over HZSM-5, *Angew. Chem. Int. Ed.* 61 (2022) e202114953, <https://doi.org/10.1002/anie.202114953>.
- C. Zhao, Y. Kou, A.A. Lemonidou, X. Li, J.A. Lercher, Highly Selective Catalytic Conversion of Phenolic Bio-Oil to Alkanes, *Angew. Chem. Int. Ed.* 48 (2009) 3987–3990, <https://doi.org/10.1002/ange.200900404>.
- J. Chang, T. Danuthai, S. Dewiyanti, C. Wang, A. Borgna, Hydrodeoxygenation of Guaiacol over Carbon-Supported Metal Catalysts, *ChemCatChem* 5 (2013) 3041–3049, <https://doi.org/10.1002/cctc.201300096>.
- K. Breitkreuz, A. Menne, A. Kraft, New process for sustainable fuels and chemicals from bio-based alcohols and acetone, *Biofuels, Bioprod. Bioref.* 8 (2014) 504–515, <https://doi.org/10.1002/bbb.1484>.
- K. Taguchi, H. Nakagawa, T. Hirabayashi, S. Sakaguchi, Y. Ishii, An Efficient Direct r-Alkylation of Ketones with Primary Alcohols Catalysed by [Ir(cod)Cl]₂/PPh₃/KOH System without Solvent, *J. Am. Chem. Soc.* 126 (2004) 72–73, <https://doi.org/10.1021/ja037552c>.
- A. Corma, T. Ródenas, M.J. Sabater, A Bifunctional Pd/MgO Solid Catalyst for the One-Pot Selective N-Monoalkylation of Amines with Alcohols, *Chem. -Eur. J.* 16 (2010) 254–260, <https://doi.org/10.1002/chem.200901501>.
- M. Sutter, N. Sotto, Y. Raoul, E. Métay, M. Lemaire, Straightforward heterogeneous palladium catalysed synthesis of aryl ethers and aryl amines via a solvent free aerobic and non-aerobic dehydrogenative arylation, *Green. Chem.* 15 (2013) 347–352, <https://doi.org/10.1039/c2gc36776a>.
- M. Sutter, R. Lafon, Y. Raoul, E. Métay, M. Lemaire, Heterogeneous palladium-catalysed synthesis of aromatic ethers by solvent-free dehydrogenative aromatisation: Mechanism, scope, and limitations under aerobic and non-aerobic conditions, *Eur. J. Org. Chem.* 26 (2013) 5902–5916, <https://doi.org/10.1002/ejoc.201300485>.
- M.-O. Simon, S.A. Girard, C.-J. Li, Catalytic aerobic synthesis of aromatic ethers from non-aromatic precursors, *Angew. Chem. Int. Ed.* 51 (2012) 7537–7540, <https://doi.org/10.1002/anie.201200698>.
- T. Nimmanwudipong, R.C. Runnebaum, K. Tay, D.E. Block, B.C. Gates, Cyclohexanone conversion catalysed by Pt/γ-Al₂O₃: Evidence of oxygen removal and coupling reactions, *Catal. Lett.* 141 (2011) 1072–1078, <https://doi.org/10.1007/s10562-011-0659-2>.
- C. Zhao, D.M. Camaioni, J.A. Lercher, Selective catalytic hydroalkylation and deoxygenation of substituted phenols to bicycloalkanes, *J. Catal.* 288 (2012) 92–103, <https://doi.org/10.1016/j.jcat.2012.01.005>.
- P. Rubio-Marqués, A. Leyva-Pérez, A. Corma, A bifunctional palladium/acid solid catalyst performs the direct synthesis of cyclohexylanilines and

- dicyclohexylamines from nitrobenzenes, *Chem. Commun.* 49 (2013) 8160–8162, <https://doi.org/10.1039/C3CC44064H>.
- [24] A. Mastalir, B. Rác, Z. Király, Á. Molnár, In situ generation of Pd nanoparticles in MCM-41 and catalytic applications in liquid phase alkyne hydrogenations, *J. Mol. Catal. A* 264 (2007) 170–178, <https://doi.org/10.1016/j.molcata.2006.09.021>.
- [25] A. Cabiac, T. Cacciaguerra, P. Trens, R. Durand, G. Delahay, A. Medevielle, D. Plée, B. Coq, Influence of textural properties of activated carbons on Pd/carbon catalysts synthesis for cinnamaldehyde hydrogenation, *Appl. Catal. A* 340 (2008) 229–235, <https://doi.org/10.1016/j.apcata.2008.02.018>.
- [26] F. Yin, S. Ji, P. Wu, F. Zhao, C. Li, Deactivation behavior of Pd based SBA-15 mesoporous silica catalysts for the catalytic combustion of methane, *J. Catal.* 257 (2008) 108–116, <https://doi.org/10.1016/j.jcat.2008.04.010>.
- [27] R. Strobel, F. Krumeich, W.J. Stark, S.E. Pratsinis, A. Baiker, Flame spray synthesis of Pd/Al₂O₃ catalysts and their behavior in enantioselective hydrogenation, *J. Catal.* 222 (2004) 307–314, <https://doi.org/10.1016/j.jcat.2003.10.012>.
- [28] J.R. Anderson, *Structure of metallic catalysts*, Academic Press, London, 1975. ISBN: 0120571501. 469 pages.
- [29] J. Ballesteros-Soberanas, A. Leyva-Pérez, Electron-Poor Phosphines Enable the Selective Semihydrogenation Reaction of Alkynes with Pd on Carbon Catalysts, *J. Phys. Chem. Lett.* 14 (2023) 965–970, <https://doi.org/10.1021/acs.jpcclett.2c03428>.
- [30] S.U. Son, Y. Jang, K.Y. Yoon, E. Kang, T. Hyeon, Facile Synthesis of Various Phosphine-Stabilized Monodisperse Palladium Nanoparticles through the Understanding of Coordination Chemistry of the Nanoparticles, *Nano Lett.* 4 (2004) 1147–1151, <https://doi.org/10.1021/nl049519>.
- [31] E. Ramirez, S. Jansat, K. Philippot, P. Lecante, M. Gomez, A.M. Masdeu-Bultó, B. Chaudret, Influence of organic ligands on the stabilization of palladium nanoparticles, *J. Organomet. Chem.* 689 (2004) 4601–4610, <https://doi.org/10.1016/j.jorganchem.2004.09.006>.
- [32] A.J. McCue, F.-M. McKenna, J.A. Anderson, Triphenylphosphine: a Ligand for Heterogeneous Catalysis Too? Selectivity Enhancement in Acetylene Hydrogenation over Modified Pd/TiO₂ Catalyst, *Catal. Sci. Technol.* 5 (2015) 2449–2459, <https://doi.org/10.1039/C5CY00065C>.
- [33] M. Guo, H. Li, Y. Ren, X. Ren, Q. Yang, C. Li, Improving catalytic hydrogenation performance of Pd nanoparticles by electronic modulation using phosphine ligands, *ACS Catal.* 8 (2018) 6476–6485, <https://doi.org/10.1021/acscatal.8b00872>.
- [34] D. Sánchez-Resa, J.A. Delgado, M.D. Fernández-Martínez, C. Didelot, A. De Mallmann, K.C. Szeto, M. Taoufik, C. Claver, C. Godard, Pd, Cu and Bimetallic PdCu NPs supported on CNTs and phosphine-functionalized silica: one-pot preparation, characterization and testing in the semi-hydrogenation of alkynes, *Eur. J. Inorg. Chem.* 47 (2021) 4970–4978, <https://doi.org/10.1002/ejic.202100806>.
- [35] L. Staiger, T. Kratky, S. Günther, O. Tomanek, R. Zboril, R.W. Fischer, R.A. Fischer, M. Cokoja, Steric and electronic effects of phosphane additives on the catalytic performance of colloidal palladium nanoparticles in the semi-hydrogenation of alkynes, *ChemCatChem* 13 (2021) 227–234, <https://doi.org/10.1002/cctc.202001121>.
- [36] M.D. Fernández-Martínez, C. Godard, Hydrogenation of CO₂ into formates by ligand-capped palladium heterogeneous catalysts, *ChemCatChem* 15 (2023) e202201408, <https://doi.org/10.1002/cctc.202201408>.
- [37] L. Wu, B.-L. Li, Y.-Y. Huang, H.-F. Zhou, Y.-M. He, Q.-H. Fan, Phosphine dendrimer-stabilized palladium nanoparticles, a highly active and recyclable catalyst for the suzuki-miyaura reaction and hydrogenation, *Org. Lett.* 8 (2006) 3605–3608, <https://doi.org/10.1021/ol0614424>.
- [38] M.A. Ortuño, N. López, Creating cavities at palladium-phosphine interfaces for enhanced selectivity in heterogeneous biomass conversion, *ACS Catal.* 8 (2018) 6138–6145, <https://doi.org/10.1021/acscatal.8b01302>.
- [39] C.H. Suresh, N. Koga, Quantifying the electronic effect of substituted phosphine ligands via molecular electrostatic potential, *Inorg. Chem.* 41 (2002) 1573–1578, <https://doi.org/10.1021/ic0109400>.
- [40] C.A. Tolman, Steric effects of phosphorus ligands in organometallic chemistry and homogeneous catalysis, *Chem. Rev.* 77 (1977) 314–348, <https://doi.org/10.1021/cr60307a002>.
- [41] J. Jover, J. Cirera, Computational assessment on the tolman cone angles for P-Ligands, *Dalton Trans.* 48 (2019) 15036–15048, <https://doi.org/10.1039/C9DT02876E>.
- [42] G. Maheut, M. Hervieu, C. Fernandez, V. Montouillout, D. Villemin, P.A. Jaffrès, Palladium complex immobilised on zirconium-phosphite: characterisation by ³¹P MAS NMR and TEM and behaviour towards reducing agents, *J. Mol. Struct.* 659 (2003) 135–142, [https://doi.org/10.1016/S0022-2860\(03\)00409-5](https://doi.org/10.1016/S0022-2860(03)00409-5).
- [43] E. Ye, H. Tan, S. Li, W.Y. Fan, Self-organization of spherical, core-shell palladium aggregates by laser-induced and thermal decomposition of [Pd(PPh₃)₄], *Angew. Chem. Int. Ed.* 45 (2006) 1120–1123, <https://doi.org/10.1002/anie.200503408>.
- [44] K. Moedritzer, L. Maier, L.C.D. Groenweghe, Phosphorus-31 Nuclear Magnetic Resonance Spectra of Phosphorus Compounds, *J. Chem. Eng. Data* 7 (1962) 307–310, <https://doi.org/10.1021/je60013a043>.
- [45] M.A. Rivero-Crespo, P. Rubio-Marqués, J.C. Hernández-Garrido, M. Mon, J. Oliver-Meseguer, A. Leyva-Pérez, Intimate ruthenium-platinum nanoalloys supported on carbon catalyse the hydrogenation and one-pot hydrogenation-coupling reaction of oxidized amino derivatives, *Catal. Sci. Technol.* 13 (2023) 2508–2516, <https://doi.org/10.1039/D2CY01846B>.
- [46] H.K. Chau, D.E. Resasco, P. Do, S. P, Acylation of m-cresol with acetic acid supported by in-situ ester formation on H-ZSM-5 zeolites, *J. Catal.* 406 (2022) 48–55, <https://doi.org/10.1016/j.jcat.2021.12.020>.